

Cite this: *Analyst*, 2022, **147**, 4073

## Construction of a HPLC-SERS hyphenated system for continuous separation and detection based on paper substrates<sup>†</sup>

Kerui Shen, Yaxian Yuan,\* Chenjie Zhang and Jianlin Yao  \*

The achievement of high-throughput separation and high-sensitivity detection of complex samples has been one of the most challenging issues in the field of analytical science. The application of a single technology alone could not satisfy the above requirements. The combination of technologies with the capability of high-efficiency separation and high-sensitivity structural-recognition is highly desired to meet the technical requirements. Herein, an automatic high-performance liquid chromatography (HPLC)-surface enhanced Raman spectroscopy (SERS) hyphenated system using paper substrates as the "interface" was constructed to achieve efficient separation and real-time detection. A homogeneous Au nanoparticle was printed on the hydrophobic filter paper with the inkjet technology. The prepared substrates served as a linkage for the continuous realization of HPLC and SERS functions. The complex system was separated by HPLC, and the effluents were loaded onto automatically and continuously replaceable paper substrates for real time SERS measurements. The continuous rapid separation and real-time detection of various two-component mixtures were achieved with the separation efficiency and detection sensitivity of each technology. The results demonstrated that the HPLC-SERS hyphenated system exhibited the complementary capability of the on-line separation and continuous structural identification of illegal additives in real samples. The detection sensitivity was increased by an order of magnitude to reach  $10^{-5}$  mol dm<sup>-3</sup>, and the efficiency and accuracy for the separation and identification on the multi-components samples were higher than those of the individual HPLC or SERS technology. It is believed that the continuous paper substrate-based HPLC-SERS hyphenated system would be developed as a promising technique for the separation and identification of multi-components mixtures with high throughput.

Received 17th June 2022,  
Accepted 2nd August 2022

DOI: 10.1039/d2an00993e  
[rsc.li/analyst](http://rsc.li/analyst)

### Introduction

The balance of high-throughput separation and high-sensitivity detection of complex samples still remains a significant challenge in the field of analysis science, involving both qualitative and quantitative analysis.<sup>1,2</sup> So far, there have been some technical difficulties in matching the above two issues simultaneously for many existing technologies and instruments.<sup>3</sup> Therefore, much effort has already been made to overcome these difficulties. The direct integration of the high-efficient separation technologies with the high-sensitive detection technologies has been one of the effective approaches. For example, Chen *et al.* developed a stable isotope labelling-assisted microfluidic chip electrospray ionization mass spectrometry platform for cell metabolism studies and drug screen-

ing processes. Multiple functional units were integrated on a chip to enrich the drug metabolites in cells and realized the ESI-Q-TOF-MS detection. Three coeluting pairs of isotopomers with an *m/z* difference of two were easily recognized and identified by chip-ESI-MS, and the detection limit of the platform for genistein was 0.2  $\mu$ M.<sup>4</sup> The combination of capillary electrophoresis with electrochemiluminescence has been explored for the separation and detection of the content of ascorbic acid (AA) in individual rat hepatocyte cells. The detection limit of AA was  $1.0 \times 10^{-8}$  M under the optimization conditions.<sup>5</sup> Although these hyphenated technologies have achieved the separation and detection of complex systems to a certain extent, the achievement of high-throughput and continuous detection is still the technical limitation.

High-performance liquid chromatography (HPLC) has attracted considerable attention due to its efficient separation performance for mixtures with different polarities.<sup>6-9</sup> Commercial HPLC detectors such as the ultraviolet visible detector (UVD) provided the absorption spectra and the corresponding retention time of each component. Unfortunately, some components are silent in UV spectroscopy, and the poor

College of Chemistry, Chemical Engineering and Materials Science, Soochow University, Suzhou 215123, China. E-mail: [yuanyaxian@suda.edu.cn](mailto:yuanyaxian@suda.edu.cn), [jlyao@suda.edu.cn](mailto:jlyao@suda.edu.cn)

<sup>†</sup> Electronic supplementary information (ESI) available: SERS spectra and chromatograms. See DOI: <https://doi.org/10.1039/d2an00993e>

structural information from UV spectra brought critical difficulties in the identification of unknown components. Moreover, mixtures with similar polarity can hardly be separated and identified by HPLC.<sup>10</sup> These problems have been resolved by combining chromatographic techniques with techniques that hold functions for the structural identification. Liquid chromatography-mass spectrometry (LC-MS) is a significant breakthrough in analysis science and is one of the generalize hyphenated systems that enables the separation of mixtures and the inferential analysis of the structure and content of each component with high specificity and sensitivity.<sup>11,12</sup> For the MS technique, the identification of components is based on the corresponding gas phase ion rather than the actual molecules.<sup>13</sup> The development of direct identification of the molecular structure for the separated components by HPLC is highly desired.

Vibrational spectroscopy provides rich spectral fingerprint information, which is considered as one of the powerful techniques to identify the molecular structure of the target as well as the concentration. In the past few decades, as a traditional vibrational spectroscopy technique, surface-enhanced Raman spectroscopy (SERS) has been developed as a direct technique for identifying molecular structures with high sensitivity up to the single molecular level.<sup>14–16</sup> In addition, one of the significant advantages of SERS is the absence from solvent effects due to their weak absorption, especially for water. This suggested that the overwhelming effect of solvents on molecular SERS signals is negligible, allowing for a higher signal-to-noise ratio in SERS spectra acquired in solution. Therefore, the hyphenated HPLC and SERS system allows for the perfectly achieved efficient separation of mixtures and the structural identification of each component. Although the foundation of HPLC and SERS occurred almost in the same period during the 1970s, the first investigation of the combination of HPLC and SERS was made by Freeman and coworkers at the end of the 1980s.<sup>17</sup> Currently, this hyphenated technique is being explored for the separation and detection of various specific components, such as pesticides, alkaloids, dyes, and drugs.<sup>18–22</sup> Based on a colloidal solution dispersed with silver halides, Schneider *et al.* constructed a layer comprising a nano-silver surface by laser photolysis as the SERS active substrate to achieve the separation and detection of heroin by HPLC-SERS system.<sup>23</sup> However, most of the studies were critically focused on the off-line mode in the early stage of the hyphenated system. It brought a significant restriction in the rapid and high throughput separation and detection. In the early 21st century, Cowcher and his coworkers reported on a hyphenated HPLC with portable Raman spectrometer for the first online separation and quantitative analysis of mixtures containing purine bases with a limit of detection of about 100–500 pmol.<sup>24</sup> In our previous studies, the HPLC-SERS hyphenated system was developed for on-line mode based on the different kinds of SERS substrates. For example, the Au nanoparticle-modified capillary was used as the on-line place for capturing the specific components from the HPLC and identifying the structure by SERS.<sup>25</sup> However, to avoid the influence of previous samples on

the next sample, it was essential to wash the capillary by NaBH<sub>4</sub> between the two detections. In the follow up investigation, replaceable SERS substrates on a manual rotating disk were used to on-line monitor reaction processes of *o*-aminothiophenol with *o*-iodobenzoyl chloride.<sup>26,27</sup> By using the magnetic Fe<sub>3</sub>O<sub>4</sub>@Ag core-shell nanoparticles as SERS substrates, the on-line detection was reached by applying a magnetic field to enrich the nanoparticles for detection. After removing the magnetic field, the enriched nanoparticles were then washed with water to eliminate the memory effect.<sup>28</sup> However, the noble metal sols or magnetic core-shell nanoparticles consistently remained on the inner wall of the test tube, generating a memory effect during the measurements.

Although the memory effect was avoided to some extent by using the above SERS substrates, the preparation of substrates was quite complicated and time-consuming. Moreover, the carrier of the SERS substrates required some manual operations, which reduced the detection accuracy. Therefore, from the viewpoint of a simple hyphenated system and low consumables, an automatic continuous on-line mode is still considered as one of the key issues for achieving the separation and detection with high throughput.

In this paper, a SERS-active substrate was fabricated by inkjet printing Au nanoparticles on a filter paper, and an automatic HPLC-SERS hyphenated system was constructed accordingly. The paper substrate is simple and efficient to prepare with relatively low cost. The flexibility of the paper substrate facilitates the construction of the automated device. The HPLC-SERS system enables the continuous separation and real-time online detection of the two-component model system. To verify the flexibility and generality of this approach, the investigation was extended to detect illegal additives of sugar-lowering drugs in health products.

## Experimental

### Materials and instrumentation

Tetrachloroauric(III) acid tetrahydrate (HAuCl<sub>4</sub>·4H<sub>2</sub>O), trisodium citrate dihydrate (Na<sub>3</sub>C<sub>6</sub>H<sub>5</sub>O<sub>7</sub>·2H<sub>2</sub>O), hydroxylamine hydrochloride (NH<sub>2</sub>OH·HCl), ammonium acetate (CH<sub>3</sub>COONH<sub>4</sub>) and 4,4'-bipyridine (BPy) were purchased from Sinopharm Chemical Reagent Co., Ltd. Polyvinylpyrrolidone (PVP, *Mw* = 10 000) was purchased from Sigma-Aldrich Co. 1,4-Benzenedithiol (BDT), *p*-nitrothiophenol (*p*NTP) and *p*-chlorobenzenethiol (*p*CBT) were purchased from TCI Co. Ltd. Alkyl ketone dimer (AKD), rosiglitazone maleate, phenformin hydrochloride and pioglitazone hydrochloride were purchased from Shanghai Yuanye Bio-Technology Co., Ltd. Methanol used in the HPLC system was of chromatographic purity. Other chemicals were of analytical reagent grade and used as received. All aqueous solutions were prepared using Milli-Q water (resistivity  $\geq$  18 M $\Omega$  cm).

Raman spectra were recorded using a confocal micro-Raman system (XploRA Plus, HORIBA Scientific). The microscope attachment used a 50 $\times$  long-distance objective. The sizes

of the slit and pinhole were 100  $\mu\text{m}$  and 300  $\mu\text{m}$ , respectively. All experiments were carried out at an excitation line of 638 nm from an internal laser. HPLC experiments were performed on a HPLC system (UltiMate<sup>TM</sup> 3000, Thermo Fisher Scientific) equipped with quaternary pump, autosampler, column thermostat, diode array detector (DAD) and Hypersil GOLD C18 column (5  $\mu\text{m}$ , 4.6 mm  $\times$  250 mm).

### Synthesis of Au nanoparticles

The 15 nm Au nanoparticles were prepared according to the Frens one-step method:<sup>29</sup> 100 mL of 0.01% (mass fraction) HAuCl<sub>4</sub> aqueous solution was heated under vigorous stirring at reflux, and 2 mL of 1% (mass fraction) citrate aqueous solution was quickly added to the solution after boiling. Then, the solution was stirred for 15 min, which gradually changed from light yellow to black, and finally to burgundy. The solution was kept boiling for 15 min, and then cooled naturally to room temperature to obtain the 15 nm Au nanoparticle solution.

The 30 nm Au nanoparticles were prepared according to the seed growth method:<sup>30</sup> 25 mL of fresh 15 nm Au nanoparticle solution, 1 mL of 1% (mass fraction) PVP aqueous solution, 1 mL of 1% (mass fraction) citrate aqueous solution, and 20 mL of 25 mM NH<sub>2</sub>OH-HCl aqueous solution were mixed and stirred gently at room temperature. Then, 20 mL of 0.1% (mass fraction) HAuCl<sub>4</sub> aqueous solution was added dropwise at a rate of 1 mL min<sup>-1</sup>. The solution gradually changed from burgundy to red. The solution was stirred for 20 min until the reaction was complete, and then the 30 nm Au nanoparticle solution was obtained.

### Hydrophobic modification of filter paper

A certain amount of 1 g dm<sup>-3</sup> AKD-heptane solution was added into a Petri dish. The filter paper was soaked in it for 30 s, then dried under 100 °C for 10 min to obtain the hydrophobic filter paper.

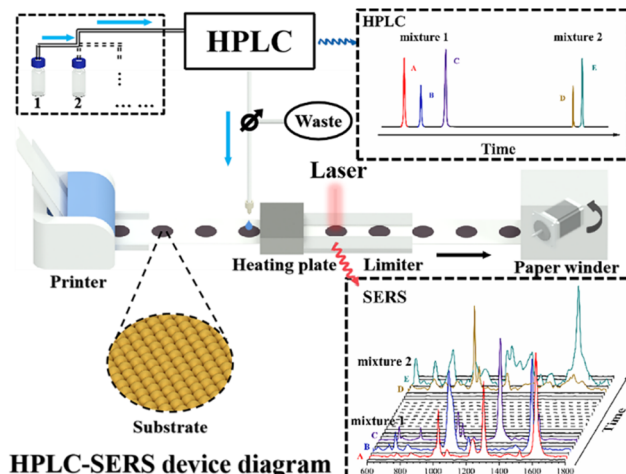
### Preparation of Au-paper substrates

The abovementioned 30 nm Au nanoparticle solution was centrifuged at 10 000 rpm for 10 min to remove 90% of the supernatant, and then cleaned and dispersed in a glycerol-ethanol solution (40% and 10% by volume) to obtain the Au-ink. The concentration of glycerol was adjusted to optimize the viscosity and surface tension.<sup>31-33</sup> The ink was injected into cartridges, which were then loaded into an HP Deskjet 3748 inkjet printer. The substrate pattern was design by Inkscape vector drawing software. Finally, the Au-ink was continuously printed on the hydrophobic filter paper 5 times to obtain the Au-paper substrate. The SEM characterization and uniformity test of the Au-paper substrate are shown in Fig. S1.†

## Results and discussion

### Construction of an automatic HPLC-SERS hyphenated system

Scheme 1 presents the schematic diagram of the HPLC-SERS hyphenated system. The “interface” between the HPLC and



Scheme 1 Schematic diagram of the HPLC-SERS hyphenated system.

SERS instruments consists of a paper SERS substrate, an auto-winder, a heating plate, and a limiter. Spaced dots (1 cm diameter circles) were printed on a long, hydrophobic roll of paper as the SERS substrates. Then, the printed substrate was loaded onto the autowinder, and a limiter was taken to hold the portion of the paper substrate to be measured under the objective of the Raman microscope. The heating plate was fixed underneath the SERS substrate to facilitate the drying rate of the solution on the SERS substrates.

Generally, HPLC mainly consists of an input injector, a separation column, mobile phase (solutions with various polarity) and a detector. The effluent liquids were divided into two separate parts for the HPLC detector and SERS measurements. Different components have their own different retention times and are successively detected in the HPLC, giving the corresponding chromatographic spectrum. Subsequently, the other effluent is added dropwise to the SERS substrate through a PTFE tube attached to the HPLC effluent liquids tube. The substrate is moved steadily through a winder to the heating plate for drying and subsequently moved to the underneath of Raman microscopy to acquire SERS spectra. As the mixture is separated by HPLC, the components with different retention times flow out one after another and interact with the surfaces of the SERS substrate to generate the corresponding SERS signals. Since the paper SERS substrate is continuously replaced in real time by the paper winder immediately after each pick-up of the effluent liquids, the memory effect of the substrate is definitely eliminated. The automatic HPLC-SERS device can be used for the continuous loading and separating of multiple samples through the column, and the real-time replacing the substrate by the winder allows for the acquirements of SERS signals from each substrate. Therefore, the HPLC and the SERS spectrum at corresponding retention times are obtained (as shown in Scheme 1). It is believed that the automatic continuous online separation and detection of multi-component samples is realized accordingly.

## Online separation and detection of a two-component model mixture

In our previous studies, 4,4'-bipyridine (BPy) and 1,4-benzene-dithiol (BDT) were selected as the probes to verify the feasibility of the HPLC-SERS hyphenated system because of their well-established SERS spectral features.<sup>25</sup> The N atoms from the pyridine compounds or S atoms from thiol compounds are adsorbed on the Au substrate surfaces to form Au–N or Au–S bonds, respectively. This bond formation is beneficial to obtain a stable SERS signal with high quality. Moreover, the conjugated benzene rings of the aromatic molecules have large scattering cross-sections. Therefore, both compounds generate strong and distinct SERS spectral features.

In the present case, BPy and BDT are mixed with a certain ratio as the model for the HPLC-SERS system. A mixture of methanol and 10 mM ammonium acetate aqueous solution (v/v 60 : 40) was used as the mobile phase with a system flow rate of 1 mL min<sup>-1</sup>. For a clear comparison, the retention times and SERS spectra with characteristic peaks of BPy and BDT were measured independently as comparison (Fig. S2 and S3†). Then, the mixture with two components was loaded into the HPLC system, and the chromatograms obtained from HPLC system are presented in Fig. 1A. Two distinct peaks at the retention time of about 4.1 min and 5.8 min were observed, and assigned to BPy and BDT, respectively. The time interval between the retention time of the two components was about 1.7 min, which is enough for the continuous SERS measurements. The corresponding SERS spectra were obtained from the effluent liquids at the retention times of 4 min and

6 min, as shown in Fig. 1B. For the former, a C–C stretching vibrational peak between the pyridine rings at 1294 cm<sup>-1</sup> and a C=C stretching vibrational peak at 1610 cm<sup>-1</sup> were detected. The same spectral features are observed in BPy (as shown in Fig. S2†), which suggested that the above SERS spectra at the retention time of 4 min originated from the BPy. A similar observation was obtained from the effluent liquids at the retention time of 6 min. Two characteristic SERS bands at 1059 cm<sup>-1</sup> and 1563 cm<sup>-1</sup> were observed, which were assigned to the C–S stretching and ring stretching vibrational modes of BDT, respectively.

The perfect match in the SERS spectral features between the single-component sample and two-component sample demonstrated that the hyphenated system exhibited the feasibility to separate and identify the mixture simultaneously. In order to further verify its capability in continuous identification, two mixed samples served as the model, including the mixture of BPy and BDT (sample 1) and the mixture of *p*-nitrothiophenol (*p*NTP) and *p*-chlorobenzenethiol (*p*CBT) (sample 2). They were continuously loaded into the HPLC-SERS hyphenated system for recording the chromatograph and SERS spectra. A mixture of methanol and 10 mM ammonium acetate aqueous solution (v/v 65 : 35) was used as the mobile phase, and the flow rate of the system was 1 mL min<sup>-1</sup>. After finishing the separation and detection of the first sample (typically about 10 min), the second sample was automatically injected for the next identification. Similarly, their respective retention times were measured independently (as shown in Fig. S4†). After comparing the features of Fig. 1A–D carefully, it should be noted that the SERS for sample 1 were

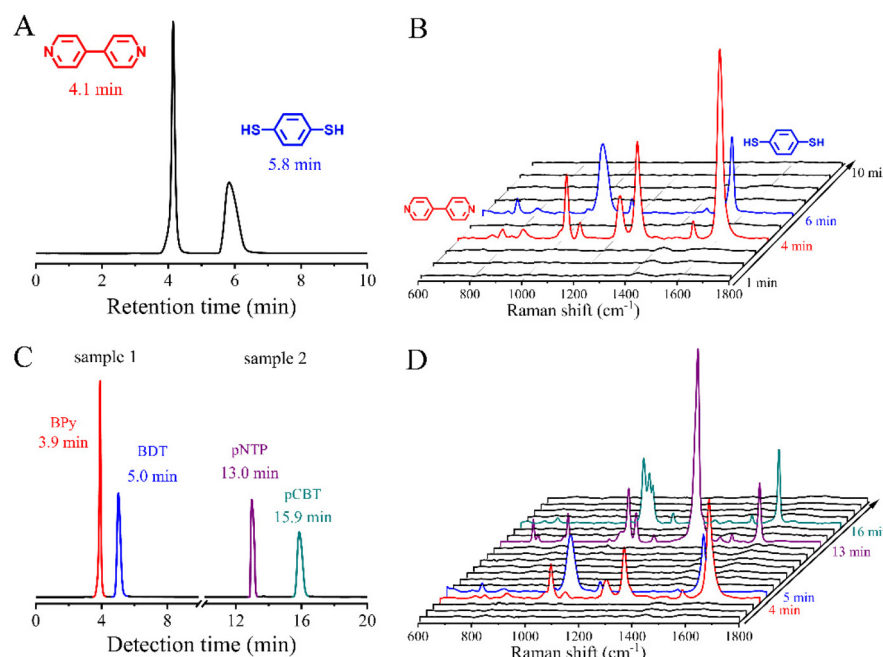


**Fig. 1** Chromatogram (A) and time-dependent SERS spectra (B) of the two-component mixture containing 4,4'-bipyridine and 1,4-benzene-dithiol. Chromatogram (C) and time-dependent SERS spectra (D) of two continuously detected two-component mixtures. The interval time is one minute. The second sample is injected immediately after the detection of the first sample is finished.

in good agreement with that observed in the simple mixture of BPy and BDT, indicating the proper operation for the hyphenated system. It is worth mentioning that the retention times of BPy and BDT were somewhat advanced due to the change of the mobile phase ratio.

Following the loading of sample 2, two chromatographic peaks at 13.0 min and 15.9 min were observed. In the corresponding SERS spectra, the characteristic peaks at 1080 and 1337  $\text{cm}^{-1}$  appeared at 13 min, corresponding to the C=S stretching vibrational mode and nitro stretching vibrational mode of pNTP, respectively, while the characteristic peaks at 1096 and 1568  $\text{cm}^{-1}$  were observed at 16 min, assigned to the chlorobenzene skeleton vibrational mode and ring stretching vibrational mode of pCBT, respectively.<sup>34,35</sup> The spectral features corresponded to those of the standard samples (as shown in Fig. S5†). The above results demonstrate the feasibility of this automatic HPLC-SERS hyphenated system for online separation and detection of multiple samples.

#### HPLC-SERS for the detection of hypoglycemic drugs

Based on the above facts, one can conclude that the construction of the continuous HPLC-SERS hyphenated system was beneficial to contribute much higher throughput in the field of analysis science, both for the standard samples and practical mixtures. Thus, it was worthy to extend the relevant application to a practical system. The hypoglycemic drugs served as the example for verify the generalization of the hyphenated system. Hypoglycemic drugs are known to be illegally mixed in the sugar-lowering health products to increase the function efficacy, causing serious harm to the health of consumers, including rosiglitazone maleate, pioglitazone hydrochloride, and phenformin hydrochloride. So far, the SERS scientific community has made a great deal of effort toward the successful development of SERS to identify different kinds of illegally added hypoglycemic drugs.<sup>36,37</sup> However, based on the nature of SERS, it still remained a significant challenge to accurately identify each component in a mixed sample. Two main facts can be attributed to the difficulty in elucidating the spectra: (i) the spectra of weak adsorption molecules were overwhelmed by stronger ones due to the competitive adsorption, (ii) the co-adsorption of multiple molecules made the spectral feature even more complicated, resulting in the difficulties in recognizing components. Therefore, it is expected that using the HPLC-SERS hyphenated system will overcome the above limitations in the identification of illegal additives.

For the accurate assignment, the SERS spectra of three typical hypoglycemic drugs, including rosiglitazone maleate, pioglitazone hydrochloride, and phenformin hydrochloride, were acquired on the Au-paper substrates (as shown in Fig. 2). Three distinct peaks at 848  $\text{cm}^{-1}$ , 1176  $\text{cm}^{-1}$  and 1607  $\text{cm}^{-1}$  in the spectrum of rosiglitazone maleate were observed, originating from the breathing vibrational mode of the benzene ring, skeleton vibrational mode of the benzene ring, and C=C stretching vibrational mode, respectively (Fig. 2a). The SERS spectrum of pioglitazone hydrochloride is presented in Fig. 2b, with the similar three peaks observed at 824, 1207,

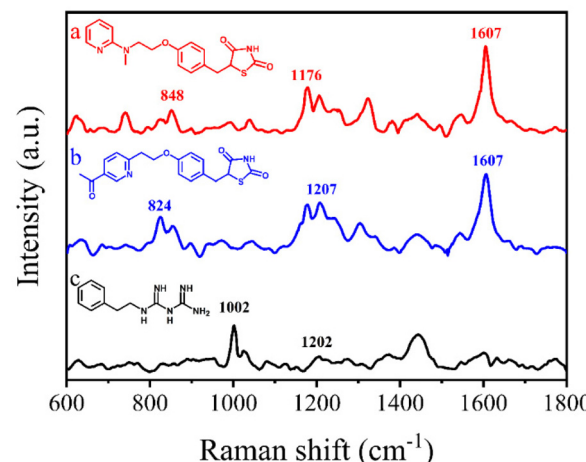
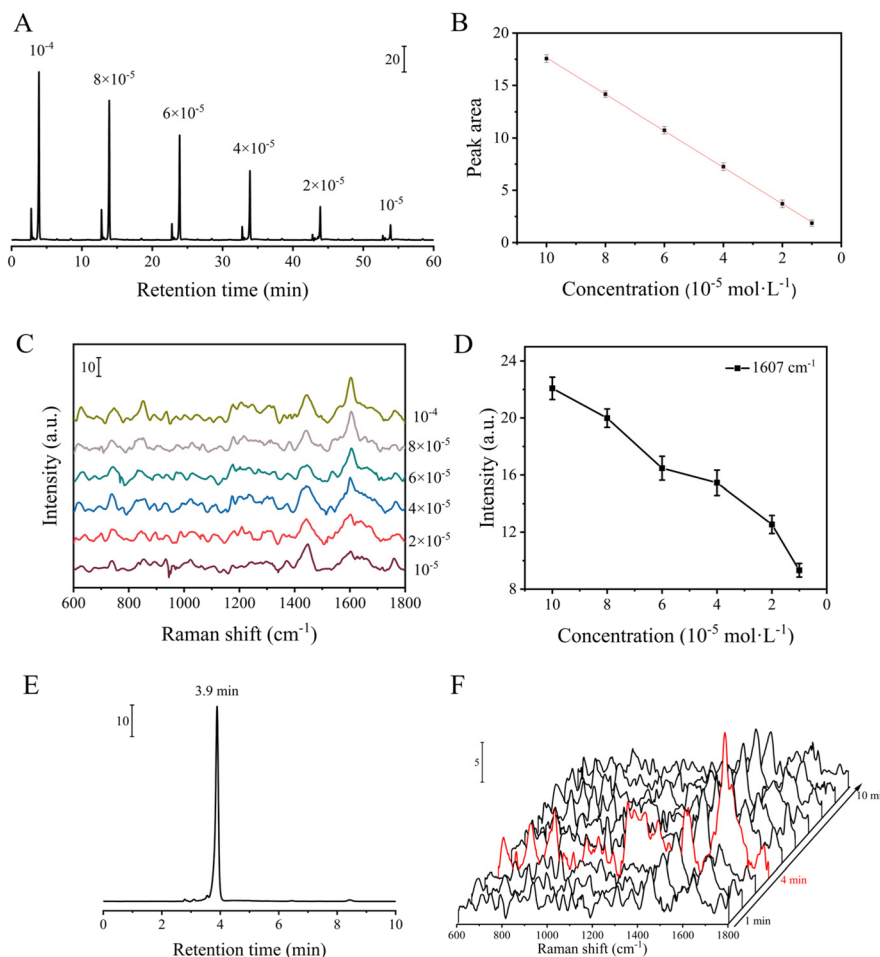


Fig. 2 SERS spectra of rosiglitazone maleate (a), pioglitazone hydrochloride (b) and phenformin hydrochloride (c) on the as-prepared Au-paper substrates.

and 1607  $\text{cm}^{-1}$ . The differences of the frequencies in the three peaks originated from the interference of the surrounding functional groups of rosiglitazone maleate and pioglitazone hydrochloride. Two peaks at 1002  $\text{cm}^{-1}$  and 1202  $\text{cm}^{-1}$  were observed, and considered as the characteristic peaks of phenformin hydrochloride.

Six rosiglitazone maleate solutions with different concentrations ( $10^{-4}$ ,  $8 \times 10^{-5}$ ,  $6 \times 10^{-5}$ ,  $4 \times 10^{-5}$ ,  $2 \times 10^{-5}$ ,  $10^{-5}$  mol  $\text{dm}^{-3}$ ) were continuously separated by HPLC, followed by the SERS detection (as shown in Fig. 3A and C). With a mixture of methanol and 10 mM ammonium acetate aqueous solution (v/v 80 : 20) as the mobile phase, six concentration-dependent chromatographic peaks appeared at the different periods, and the appearance time was dependent on the processes of the continuous injection, *i.e.*, the interval time of peaks was not changed and the peak features were very similar. The corresponding SERS spectra at the period of the chromatographic peaks were extracted from the series of continuous detection (as shown in Fig. 3C). The band at about 1450  $\text{cm}^{-1}$  originated from the background of the paper substrate. The characteristic peaks at 848  $\text{cm}^{-1}$ , 1176  $\text{cm}^{-1}$  and 1607  $\text{cm}^{-1}$  observed in the SERS spectra were almost identical to those of the standard sample (as shown in Fig. 2a and 3C), indicating that rosiglitazone was present in the effluent associated with the chromatographic peaks. The area of each peak in the chromatogram was related to the concentration. Thus, the peak area ( $A$ ) *versus* concentration ( $C$ ) curve was obtained accordingly, indicating the perfect linear relationship with the fitted result of  $A = C \times 174.211.0239 + 0.2147$  (as shown in Fig. 3B). Taking the characteristic peak of rosiglitazone at 1607  $\text{cm}^{-1}$  as an example, the peak intensities were also positively correlated with the concentration (as shown in Fig. 3D). However, it should be pointed out that the linearity of the SERS intensity-concentration was poorer than that of HPLC. It was mainly due to the nature of SERS as a semi-quantitative analysis tool. The above experimental facts indicated that the HPLC-SERS hyphenated



**Fig. 3** Chromatogram (A) and SERS spectra (C) of rosiglitazone maleate at different concentrations. (B) HPLC standard curve of rosiglitazone maleate. (D) Relation curve between the SERS intensity and concentration of rosiglitazone maleate. Chromatogram (E) and time-dependent SERS spectra (F) of the rosiglitazone tablet. The interval time is one minute.

system provided a platform for the identification of components with higher throughput. In order to verify the above assumption, it was extended to a commercial sample. One tablet (4 mg) of commercially available rosiglitazone tablet was dissolved in 250 ml of methanol (calculated concentration of  $\sim 4.48 \times 10^{-5}$  mol dm<sup>-3</sup>). Then, the solution was injected into the HPLC-SERS hyphenated system for the identification of the concentration, as well as the structure (as shown in Fig. 3E and F). A peak appeared in the chromatogram at the retention time of 3.9 min, and characteristic peaks at 848 cm<sup>-1</sup>, 1176 cm<sup>-1</sup> and 1607 cm<sup>-1</sup> were observed in the corresponding SERS spectrum. The very similar HPLC peak associated with the same SERS spectral feature indicated unambiguously that the target substance was rosiglitazone. Based on the peak areas in the chromatogram and A-C curve, the concentration of rosiglitazone could be found to be  $\sim 4.44 \times 10^{-5}$  mol dm<sup>-3</sup>, which is close to the calculation result. The above results demonstrate that this automatic HPLC-SERS hyphenated system can simultaneously perform qualitative and quantitative analyses of samples with high throughput.

### Identification of illegal addition in health products

In order to identify the illegal addition of drugs in hypoglycemic supplements, the practical health products were spiked with the target component. A certain amount of individual hypoglycemic drug rosiglitazone maleate (calculated concentration of about 10<sup>-4</sup> mol dm<sup>-3</sup>) was firstly added to the supplements (bitter gourd buckwheat mulberry leaf capsules) and extracted with methanol. Briefly, the content of a capsule (about 0.29 g) was weighed and mixed with a certain amount of rosiglitazone maleate (about 0.47 mg), then dissolved in 10 ml methanol, and the supernatant was extracted by ultrasonication to obtain the drug extract. The extract solution was then introduced into the HPLC-SERS hyphenated system to record the chromatograms and SERS spectra, respectively, and the same measurements were performed on the blank sample without the hypoglycemic agent (as shown in Fig. 4A). Besides the chromatographic peak of the health product with the retention time of about 3 min, a new peak appeared at about 4 min in the spiked sample, which originated from the separ-

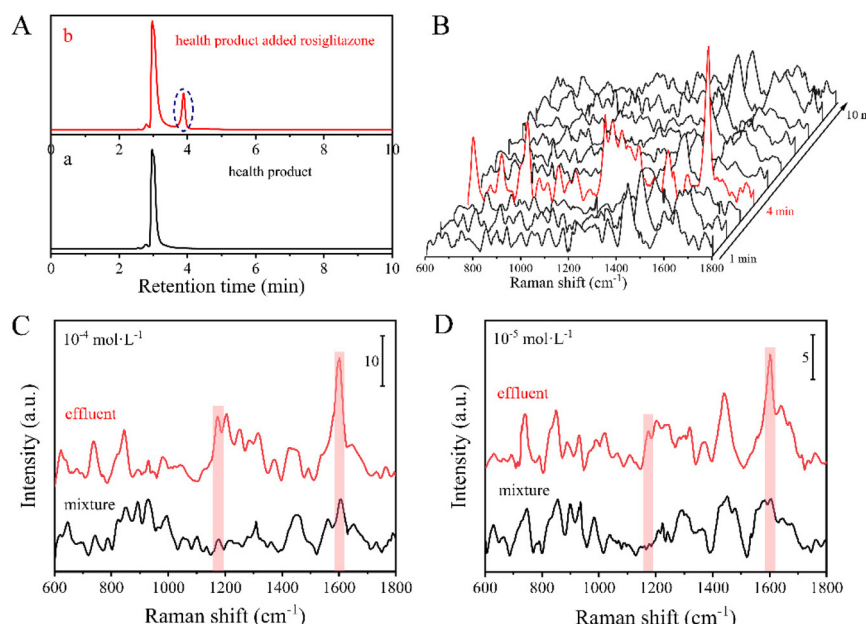


**Fig. 4** (A) Chromatograms of health products with (b) and without rosiglitazone (a). (B) Time-dependent SERS spectra of health products spiked with rosiglitazone. The interval time is one minute. Mixture and effluent of health products containing rosiglitazone at a concentration of  $10^{-4}$  mol dm<sup>-3</sup> (C) and  $10^{-5}$  mol dm<sup>-3</sup> (D).

ated rosiglitazone molecules. Correspondingly, the SERS peaks at  $848\text{ cm}^{-1}$ ,  $1176\text{ cm}^{-1}$  and  $1607\text{ cm}^{-1}$  were detected at the retention time of 4 min, and the good match in the spectral features suggested the existence of rosiglitazone in the effluent. The above results demonstrated that the HPLC-SERS hyphenated system ran properly in the practical samples. After the concentration of rosiglitazone maleate was decreased to  $10^{-4}\text{ mol dm}^{-3}$ , only weak characteristic peaks at  $1176\text{ cm}^{-1}$  and  $1607\text{ cm}^{-1}$  were observed by the direct SERS measurements on the mixture (as shown in Fig. 4C). However, the rosiglitazone molecules could be clearly recognized after separation according to the observable SERS peaks. It was reasonable to assume that the HPLC-SERS hyphenated system improved the capability in recognizing the target molecule in a complex system. Upon further decreasing the concentration of rosiglitazone maleate to  $10^{-5}\text{ mol dm}^{-3}$  (as shown in Fig. 4D), it was hard to observe any characteristic peak in the SERS spectrum, as it was overwhelmed by the noise of the substrate itself. However, the SERS peaks, assigned to the characteristic peaks of rosiglitazone maleate, were ambiguously detectable at  $1176\text{ cm}^{-1}$  and  $1607\text{ cm}^{-1}$  after separation by the hyphenated system. Therefore, based on the complementary strategies of HPLC and SERS, the detection sensitivity and capability in the structural recognition were obviously improved by comparison to the performance of the single individual technologies.

To further develop the advantages of the HPLC-SERS hyphenated technique on the detection of illegal addition in health products, a variety of different hypoglycemic agents were introduced to the contents of two health products, respectively. They were extracted by methanol, and then two samples were successively loaded into the HPLC-SERS hyphenated system

for detection. A mixture of methanol and 10 mM ammonium acetate aqueous solution (v/v 65 : 35) was used as the mobile phase, and the flow rate of the system was  $0.9\text{ mL min}^{-1}$ . The detection time of each sample was 10 min, and the second sample was automatically injected and identified immediately after finishing the first sample. As shown in the chromatogram in Fig. 5A, besides the peaks of the health product, new peaks were observed at 7.1 min and 8.0 min for sample 1, and 14.0 min and 17.1 min for sample 2, which corresponded to the retention times of their respective detections (as shown in Fig. S6†). It should be noted that the proportion of aqueous solution in the mobile phase was increased from 20% to 35%, and the retention time of rosiglitazone was also delayed from 3.9 minutes (Fig. 3) to 7.1 minutes (Fig. 5) accordingly. At the same time, distinct peaks were observed at  $848\text{ cm}^{-1}$ ,  $1176\text{ cm}^{-1}$ ,  $1607\text{ cm}^{-1}$  and  $824\text{ cm}^{-1}$ ,  $1207\text{ cm}^{-1}$ ,  $1607\text{ cm}^{-1}$  in the SERS spectra at 7 min and 8 min, which corresponded to the SERS signals of rosiglitazone and pioglitazone, respectively, indicating that rosiglitazone maleate and pioglitazone hydrochloride were included in sample 1. In sample 2, peaks were observed at  $1002\text{ cm}^{-1}$ ,  $1202\text{ cm}^{-1}$  and  $848\text{ cm}^{-1}$ ,  $1176\text{ cm}^{-1}$ ,  $1607\text{ cm}^{-1}$  in the SERS spectra at 14 min and at 17 min, which corresponded to the SERS signals of phenformin and rosiglitazone, respectively, indicating that the hypoglycemic agents added to sample 2 were phenformin hydrochloride and rosiglitazone maleate. These results demonstrated that the automatic HPLC-SERS system exhibited the on-line and continuous performance in the separation and identification. The complementary functions of HPLC and SERS allowed for the improvement of the capability in recognizing multiple unknown component mixtures with high throughput.

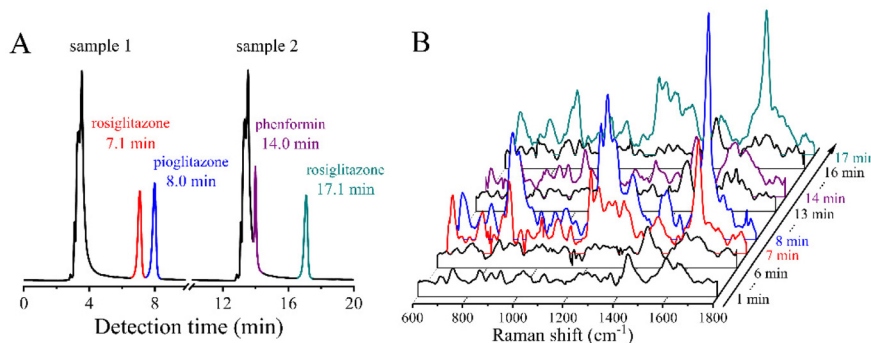


**Fig. 5** Chromatogram (A) and time-dependent SERS spectra (B) of two continuously detected health product samples. The interval time is one minute. The second sample is injected immediately after the detection of the first sample is finished.

## Conclusions

In summary, the performance of the continuous identification of the home-made HPLC-SERS hyphenated system was improved through the introduction of an automatic scrolled paper substrate. The feasibility of the HPLC-SERS system was verified by the on-line separation and detection of the two-component model system, and the system was successfully extended to the application in identifying the illegally added hypoglycemic drugs in the practical dietary supplements. The results demonstrated that the HPLC-SERS hyphenated system exhibited the complementary capability of on-line separation and continuous structural identification for the illegal additive in real samples. The detection sensitivity was increased by an order of magnitude, and the efficiency and accuracy for the separation and identification of the multi-component samples were higher than those of the individual HPLC or SERS technologies. Based on the above facts, it is believed that the continuous paper substrate-based HPLC-SERS hyphenated system could be a promising technique for the separation and identification on the multi-components mixtures with high throughput.

## Conflicts of interest

There are no conflicts to declare.

## Acknowledgements

This work was supported by the National Natural Science Foundation of China (No. 22172109, 21773166), Key Program Natural Science Research Project of Jiangsu Colleges and Universities (18KJA150009, 21KJA150009), and Project of Scientific and Technologic Infrastructure of Suzhou (SZS201708).

## Notes and references

1 Q. Wu, H. M. Yuan, L. H. Zhang and Y. K. Zhang, *Anal. Chim. Acta*, 2012, **731**, 1–10.

- 2 A. Subaihi, D. K. Trivedi, K. A. Hollywood, J. Bluett, Y. Xu, H. Muhamadali, D. I. Ellis and R. Goodacre, *Anal. Chem.*, 2017, **89**, 6702–6709.
- 3 W. A. Hassanain, E. L. Izake, A. Sivanesan and G. A. Ayoko, *J. Pharm. Biomed. Anal.*, 2017, **136**, 38–43.
- 4 Q. S. Chen, J. Wu, Y. D. Zhang and J. M. Lin, *Anal. Chem.*, 2012, **84**, 1695–1701.
- 5 X. M. Sun, Y. Niu, S. Bi and S. S. Zhang, *Electrophoresis*, 2008, **29**, 2918–2924.
- 6 A. L. Robinson, *Science*, 1979, **203**, 1329–1332.
- 7 M. Arabi, A. Ostovan, A. R. Bagheri, X. T. Guo, J. H. Li, J. P. Ma and L. X. Chen, *Talanta*, 2020, **215**, 120933.
- 8 H. Jiang, K. W. Yang, X. X. Zhao, W. Q. Zhang, Y. Liu, J. W. Jiang and Y. Cui, *J. Am. Chem. Soc.*, 2021, **143**, 390–398.
- 9 K. Hu, Y. M. Shi, W. X. Zhu, J. L. Cai, W. J. Zhao, H. H. Zeng, Z. Q. Zhang and S. S. Zhang, *Food Chem.*, 2021, **339**, 128079.
- 10 J. C. Lindon, J. K. Nicholson and I. D. Wilson, *J. Chromatogr. B: Anal. Technol. Biomed. Life Sci.*, 2000, **748**, 233–258.
- 11 M. Araya-Farias, A. Gaudreau, E. Rozoy and L. Bazinet, *J. Agric. Food Chem.*, 2014, **62**, 4241–4250.
- 12 Y. S. Huang, T. Shi, X. Luo, H. L. Xiong, F. F. Min, Y. Chen, S. P. Nie and M. Y. Xie, *Food Chem.*, 2019, **275**, 255–264.
- 13 J. W. Martin, K. Kannan, U. Berger, P. De Voogt, J. Field, J. Franklin, J. P. Giesy, T. Harner, D. C. G. Muir, B. Scott, M. Kaiser, U. Jarnberg, K. C. Jones, S. A. Mabury, H. Schroeder, M. Simcik, C. Sottani, B. Van Bavel, A. Karrman, G. Lindstrom and S. Van Leeuwen, *Environ. Sci. Technol.*, 2004, **38**, 248a–255a.
- 14 S. M. Nie and S. R. Emery, *Science*, 1997, **275**, 1102–1106.
- 15 K. Kneipp, Y. Wang, H. Kneipp, L. T. Perelman, I. Itzkan, R. Dasari and M. S. Feld, *Phys. Rev. Lett.*, 1997, **78**, 1667–1670.
- 16 J. F. Li, Y. F. Huang, Y. Ding, Z. L. Yang, S. B. Li, X. S. Zhou, F. R. Fan, W. Zhang, Z. Y. Zhou, D. Y. Wu, B. Ren, Z. L. Wang and Z. Q. Tian, *Nature*, 2010, **464**, 392–395.
- 17 R. D. Freeman, R. M. Hammaker, C. E. Meloan and W. G. Fateley, *Appl. Spectrosc.*, 1988, **42**, 456–460.

18 R. S. Sheng, F. Ni and T. M. Cotton, *Anal. Chem.*, 1991, **63**, 437–442.

19 B. Sagmuller, B. Schwarze, G. Brehm, G. Trachta and S. Schneider, *J. Mol. Struct.*, 2003, **661**, 279–290.

20 C. Carrillo-Carrion, S. Armenta, B. M. Simonet, M. Valcarcel and B. Lendl, *Anal. Chem.*, 2011, **83**, 9391–9398.

21 C. Carrillo-Carrion, B. M. Simonet, M. Valcarcel and B. Lendl, *J. Chromatogr. A*, 2012, **1225**, 55–61.

22 C. Zaffino, G. D. Bedini, G. Mazzola, V. Guglielmi and S. Bruni, *J. Raman Spectrosc.*, 2016, **47**, 607–615.

23 G. Trachta, B. Schwarze, B. Sagmuller, G. Brehm and S. Schneider, *J. Mol. Struct.*, 2004, **693**, 175–185.

24 D. P. Cowcher, R. Jarvis and R. Goodacre, *Anal. Chem.*, 2014, **86**, 9977–9984.

25 W. Wang, M. M. Xu, Q. H. Guo, Y. X. Yuan, R. N. Gu and J. L. Yao, *RSC Adv.*, 2015, **5**, 47640–47646.

26 C. L. Jiao, W. Wang, J. Liu, Y. X. Yuan, M. M. Xu and J. L. Yao, *Acta Chim. Sin.*, 2018, **76**, 526–530.

27 H. Zhang, C. J. Zhang, M. M. Xu, Y. X. Yuan and J. L. Yao, *Chem. J. Chin. Univ.*, 2020, **41**, 2496–2502.

28 J. Liu, H. L. Sun, L. Yin, Y. X. Yuan, M. M. Xu and J. L. Yao, *Acta Chim. Sin.*, 2019, **77**, 257–262.

29 G. Frens, *Nature (London), Phys. Sci.*, 1973, **241**, 20–22.

30 P. P. Fang, J. F. Li, Z. L. Yang, L. M. Li, B. Ren and Z. Q. Tian, *J. Raman Spectrosc.*, 2008, **39**, 1679–1687.

31 W. W. Yu and I. M. White, *Analyst*, 2013, **138**, 1020–1025.

32 E. P. Hoppmann, W. W. Yu and I. M. White, *Methods*, 2013, **63**, 219–224.

33 E. P. Hoppmann, W. W. Yu and I. M. White, *IEEE J. Sel. Top. Quantum Electron.*, 2014, **20**, 7300510.

34 B. O. Skadtchenko and R. Aroca, *Spectrochim. Acta, Part A*, 2001, **57**, 1009–1016.

35 J. L. Chen, T. Wu and Y. W. Lin, *Microchem. J.*, 2018, **138**, 340–347.

36 Y. Zhang, X. Y. Huang, W. F. Liu, Z. N. Cheng, C. P. Chen and L. H. Yin, *Anal. Sci.*, 2013, **29**, 985–990.

37 R. Q. Lu, Z. K. Qi, S. Y. Wang, X. G. Tian and X. Y. Xu, *Microchem. J.*, 2021, **169**, 106523.